water

MDPI

Article

Determination of Growth Stage-Specific Crop Coefficients (K_c) of Sunflowers (*Helianthus annuus* L.) under Salt Stress

Minghai Hong [1], Wenzhi Zeng [1,2,3,*], Tao Ma [1], Guoqing Lei [1], Yuanyuan Zha [1], Yuanhao Fang [4], Jingwei Wu [1] and Jiesheng Huang [1]

1 State Key Laboratory of Water Resources and Hydropower Engineering Science, Wuhan University, Wuhan 430072, China; hongminghai1992@whu.edu.cn (M.H.); maxman@whu.edu.cn (T.M.); Leiguoqing1001@whu.edu.cn (G.L.); zhayuan87@whu.edu.cn (Y.Z.); wujingweiwhu@gmail.com (J.W.); huangjiesheng1962@gmail.com (J.H.)
2 Crop Science Group, Institute of Crop Science and Resource Conservation (INRES), University of Bonn, Katzenburgweg 5, D-53115 Bonn, Germany
3 State Key Laboratory of Hydrology-Water Resources and Hydraulic Engineering, Hohai University, Nanjing 210098, China
4 Department of Hydrology and Water Resources, Hohai University, Nanjing 210098, China; yuanhao.fang@outlook.com
* Correspondence: zengwenzhi1989@whu.edu.cn or wzeng@uni-bonn.de; Tel.: +86-27-6877-2215

Academic Editor: Ranka Junge
Received: 16 January 2017; Accepted: 9 March 2017; Published: 13 March 2017

Abstract: Crop coefficients (K_c) are important for the development of irrigation schedules, but few studies on K_c focus on saline soils. To propose the growth-stage-specific K_c values for sunflowers in saline soils, a two-year micro-plot experiment was conducted in Yichang Experimental Station, Hetao Irrigation District. Four salinity levels including non-salinized (EC_e = 3.4–4.1 dS·m^{-1}), low (EC_e = 5.5–8.2 dS·m^{-1}), moderate (EC_e = 12.1–14.5 dS·m^{-1}), and high (EC_e = 18.3–18.5 dS·m^{-1}) levels were arranged in 12 micro-plots. Based on the soil moisture observations, Vensim software was used to establish and develop a physically-based water flow in the soil-plant system (WFSP) model. Observations in 2012 were used to calibrate the WFSP model and acceptable accuracy was obtained, especially for soil moisture simulation below 5 cm ($R^2 > 0.6$). The locally-based K_c values (LK_c) of sunflowers in saline soils were presented according to the WFSP calibration results. To be specific, LK_c for initial stages (K_{c1}) could be expressed as a function of soil salinity (R^2 = 0.86), while R^2 of LK_c for rapid growth (K_{c2}), middle (K_{c3}), and mature (K_{c4}) stages were 0.659, 1.156, and 0.324, respectively. The proposed LK_c values were also evaluated by observations in 2013 and the R^2 for initial, rapid growth, middle, and mature stages were 0.66, 0.68, 0.56 and 0.58, respectively. It is expected that the LK_c would be of great value in irrigation management and provide precise water application values for salt-affected regions.

Keywords: crop coefficient; modeling; salinity; sunflowers; Vensim

1. Introduction

Sunflower (*Helianthus annuus* L.) is one of the four most important oil crops in the world [1]. Based on data from the National Sunflower Association, more than 25 million hectares of global croplands are planted in sunflowers. The Hetao Irrigation District, which is located in northern China, is the largest sunflower-growing region in China, and sunflower seeds are the main source of income for local farmers [2]. However, due to high rates of evaporation and low levels of precipitation, the significance of irrigation in attaining and sustaining optimum productivity of major crops in the Hetao Irrigation

District or other regions with similar climate conditions is important and has been documented [3,4]. Demir et al. [1] reported that the seed and oil yield of oil sunflowers increased by 82.9% and 85.4% with irrigation as compared to the treatment without irrigation at three growth stages of sunflowers in Turkey; Ertek and Kara [5] also conducted a series of deficit irrigation experiments, and concluded that maize fresh ear yield was affected by water stress. Furthermore, between yield and water use, a positive linear relationship has been recognized by various researchers [6–10]. However, because of the limited knowledge of crop water use in this region, flood irrigation without scheduling is still the main irrigation practice, which is not only a non-efficient use of water resources but also has the possibility for increasing the risk of groundwater contamination because a large number of solutes could be leached below the root zone using this irrigation practice [11]. Therefore, it is necessary to determine an efficient and representative irrigation scheduler to improve the crop productivity and water resource management for the region.

Crop evapotranspiration (ET_c), which represents the combined processes of water loss through evaporation from soil surface and transpiration from crop surface, has a potential advantage to attain proper irrigation scheduling [12,13]. Although there are few traditional technologies (e.g., weighting lysimeters, sap-flow sensors) that can assist scientists with determining ET_c [14], it is still laborious, time-consuming and costly to apply these technologies in large regions [15]. As recommended by Food and Agricultural Organization (FAO) [16], the approach of the crop coefficient (K_c) is widely used to estimate crop water use and to schedule irrigations. The concept of K_c was introduced by Jensen [17] and further developed by the other researchers [16,18,19]. Generally speaking, K_c is defined as the ratio between ET_c and reference evapotranspiration (ET_0) which is based on the evapotranspiration (ET) rate from a well-water (not limiting) reference surface. As discussed and summarized in the FAO document, the single crop coefficient approach is used for most applications related to irrigation planning, design, and management due to its simplicity. Values of K_c for most agricultural crops increase from a minimal value at planting to a maximum K_c value near full canopy cover or pollination. FAO provides details on the development and use of generalized K_c values for different crops in different regions of the world [16]. However, few methods available to attain crop coefficients for site-specific values have been determined experimentally for different growth stages of sunflowers. What data is available is considerably different from that listed in the FAO-56 paper [20]. Meanwhile, approximately 70% of the cultivated land in the Hetao Irrigation District is contaminated by soil salinity, which has been proven to be a vital factor affecting crop growth [3,21]. Based on our previous works, soil salinity affects sunflower growth elements such as the photosynthesis [22] and dry matter formation [23], which indicates that there may be a direct relationship between soil salinity and K_c. However, as far as we know, almost no published studies focus on this correlation. Therefore, it is important to determine local-based K_c values for more precise crop ET_c estimation, especially for crops growing in saline soils. However the traditional method for estimating K_c is usually via weighting lysimeters [24], which is both costly and time consuming. Due to the lack of research-based information on sunflower water use in saline soils and the inconvenience of directly experimental K_c determination, the objectives of this study were to (1) construct a physically-based model to determine local growth-stage-specific K_c values for sunflowers in different levels of saline soils, and (2) to ascertain the relationship between K_c values and soil salinity (K_c-S). Also, evaluations for both model performance and the K_c-S relationship were performed based on field experiments.

2. Materials and Methods

2.1. Study Site Characteristics and Field Experiment Design

This experiment was conducted at the Yichang Experimental Station in the Hetao Irrigation District (40°19′ to 41°18′ N, 106°20′ to 109°19′ E), Inner Mongolia, China (Figure 1a). The Hetao Irrigation District has the largest gravity irrigation area (~1.05×10^6 ha) in China and is representative of the continental climate. The mean annual precipitation and mean annual

potential evapotranspiration are approximately 176 mm and 2056 mm, respectively, and 63%–70% of precipitation is from June to August [4]. Micro-plot experiments were conducted on sunflowers (*Helianthus*) for two years, in 2012 and 2013. Each micro-plot covered an area of 1.8 m × 1.8 m and was surrounded by an impermeable plastic barrier to a depth of 1.5 m to prevent lateral drainage (Figure 1b,c). Salt crusts on the surface of saline bare soils were collected and used to modify salinity from the 0–20 cm depth of the micro-plots. Saturated electrical conductivity (EC_e) was used to indicate soil salinity levels. Four different salinity levels were established, including non-salinized (EC_e = 3.4–4.1 dS·m^{-1}), low (EC_e = 5.5–8.2 dS·m^{-1}), moderate (EC_e = 12.1–14.5 dS·m^{-1}), and high (EC_e = 18.3–18.5 dS·m^{-1}), respectively. Sunflowers (cv. LD5009) were planted on 7 June 2012 and 4 June 2013 in a grid of four rows (0.45 m × 0.4 m spacing) within each subplot (Figure 1d); the plant density was 4.94 plants m^{-2}, and soil was covered by plastic films in order to decrease soil evaporation. Plants were harvested on 24 September 2012 and 16 September 2013. More details for the micro-plot experiments can be found in [21]. Sunflower growth periods were divided into four stages including initial stage, rapid growth stage, middle stage, and mature stage [25]. Soil samples at different depths were taken at sowing stage and four times for each subsequent growth stage. Soil samples were taken at depths of 0–5, 5–10, 10–20, 20–40, 40–60, 60–80, and 80–100 cm on 10 June, 13 July, 2 August, 9 August, and 24 September in 2012 and at depths of 0–10, 10–20, 20–30, 30–40, 40–60, 60–80, 80–100 cm on 30 May, 10 July, 24 July, 14 August, and 16 September in 2013, respectively. After sampling, soil moisture was determined using the oven-dry method. Soil texture was analyzed using the pipette method [26,27] and the bulk density was measured by the cutting-ring method [27,28] (Table 1).

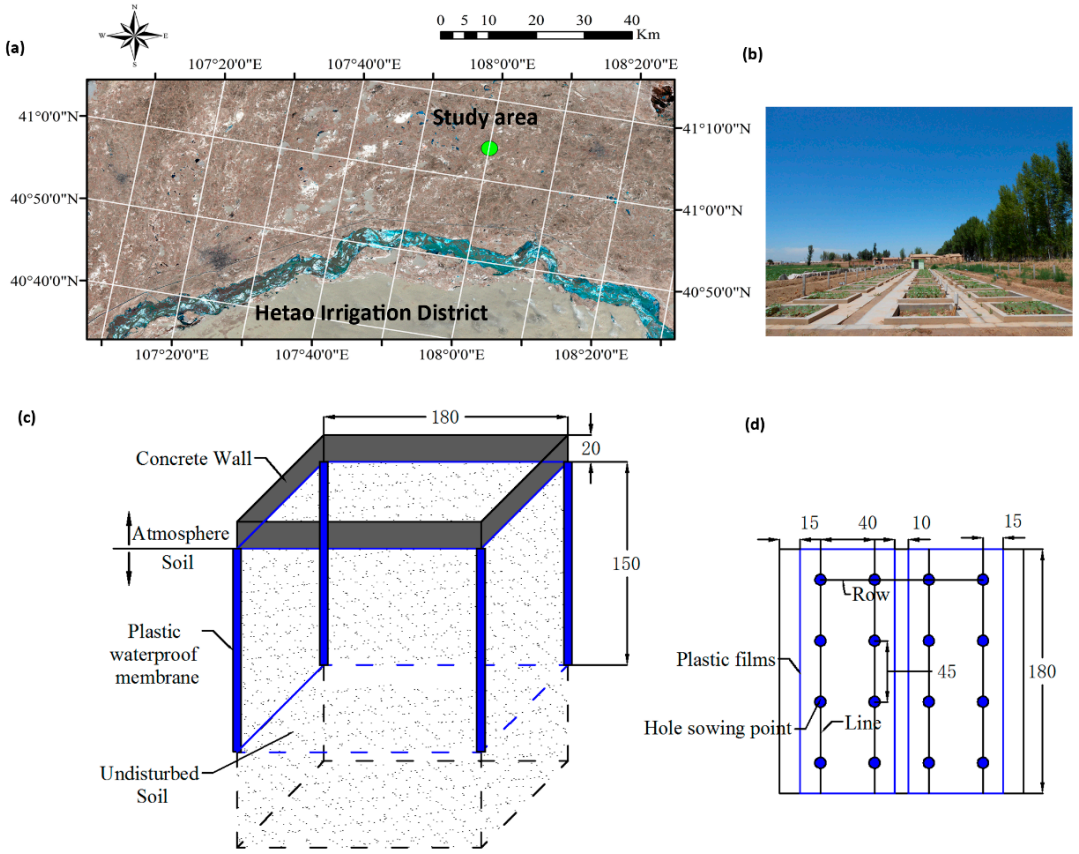

Figure 1. The location site (**a**) of the experimental study area. The green dot is the location of subplots at the Yichang Experimental Station. The arrangement of the trial blocks are depicted in (**b**) with the schematic diagram of the block profile (**c**) and plant arrangement (**d**) within each block (units in cm) also being shown.

Table 1. Soil physical properties of experimental area.

Depth (cm)	Soil Particle Size Distribution/Mean ± S.D.* (%)			Bulk Density (g/cm^3)
	Sand (0.05–2.0 mm)	Silt (0.002–0.05 mm)	Clay (< 0.002 mm)	
0–10	12.58 ± 4.30	54.94 ± 12.13	32.48 ± 13.86	1.35
10–20	11.79 ± 3.97	52.81 ± 13.53	35.40 ± 14.67	1.35
20–30	12.02 ± 4.24	52.32 ± 12.43	35.66 ± 14.05	1.35
30–40	12.27 ± 6.86	53.77 ± 12.10	33.96 ± 15.49	1.44
40–60	8.91 ± 12.96	69.77 ± 11.41	21.32 ± 12.29	1.48
60–80	12.48 ± 13.91	70.57 ± 11.80	16.95 ± 10.61	1.51
80–100	16.69 ± 16.69	69.59 ± 13.28	13.72 ± 6.17	1.51

Note: * S.D. indicates standard deviation.

2.2. Model Descriptions

System Dynamics (SD) was firstly proposed by Forrester [29] and widely applied to analyze the change of a modeling system based on the linkage and response mechanism among models, which can represent complex systems and analyze their dynamic behavior [30]. Vensim software (http://vensim.com/) has been shown to be an adequate tool to depict system dynamics [31–33]. Vensim™, the Ventana® Simulation Environment, is an interactive software environment that allows the development, exploration, analysis and optimization of simulation models. It was created to increase the capabilities and productivity of skilled modelers and has the functionality that improves the quality and understanding of models [34]. In this study, Vensim software was used to establish a physically-based model to consider the water flow in the soil–plant system (WFSP model). Vensim is designed to simultaneously solve a series of material held within a stock and its depletion or replenishment by flow into and out of the stock [35,36], and its open version Vensim PLE is freely available to the academic community for use in education and research. Here, stocks represent the mass of water within a given soil layer; while the flows represent the fluxes of water among stocks, model runs were conducted using a one-day time step, with state variables at each interval. All storage terms were given in millimeters; also, flow terms were given in millimeters per day. More details about this model, including the equations used to calculate the stocks and the flows are shown in following sections.

2.2.1. Basic Principles

Figure 2 indicates the water movement in the root zone of sunflowers for our model. Based on our soil sampling design, we considered a 100-cm depth soil profile and divided it into seven layers (0–5, 5–10, 10–20, 20–40, 40–60, 60–80, and 80–100 cm, for 2012 and for 2013, 0–10, 10–20, 20–30, 30–40, 40–60, 60–80, and 80–100 cm).

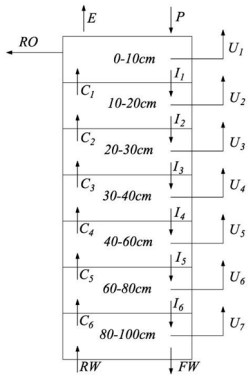

Figure 2. Basic model framework. P is precipitation (mm); C is the capillary water movement into the soil layer (mm); I is the seepage movement out of the soil layer (mm); E is soil evaporation (mm); and U is root water uptake from the soil layer (mm). RO is the surface runoff (mm). RW is the groundwater recharge (mm); FW is the water flow out of the whole root zone (mm). Subscript i indicates the layer number.

For the layer 1, layers 2–6, and layer 7, we can describe the water movement by Equations (1)–(3) respectively.

$$\Delta S_1 = S_{1,t} - S_{1,t-1} = P + C_1 - RO - U_1 - I_1 - E \quad (1)$$

$$\Delta S_i = S_{i,t} - S_{i,t-1} = C_i + I_{i-1} - C_{i-1} - U_i - I_i \quad (2)$$

$$\Delta S_7 = S_{7,t} - S_{7,t-1} = I + RW - FW - U_7 - C_6 \quad (3)$$

where S is soil water storage within every soil layer (subscript i represents a soil layer) (mm), P is precipitation (mm); C is the capillary water movement into the soil layer (mm); I is the seepage movement out of the soil layer (mm); E is soil evaporation (mm); and U is root water uptake from the soil layer (mm). RO is the surface runoff (mm), and because of the scarce precipitation in Hetao District, RO equals zero; RW is the groundwater recharge (mm); FW is the water flow out of the whole root zone (mm) and ΔS is the change of water storage for the specific soil layer (mm) during the time interval. Subscript t indicates the current moment (day) and $t - 1$ indicates the last moment (day). Subscript i indicates the layer number (from 2 to 6).

2.2.2. Infiltration

Infiltration is described based on Kostiakov [37] model (Equation (4)).

$$i_t = i_1 t^{-p} \quad (4)$$

where i_t is the infiltration rate at time t (h) and expressed using the infiltration depth at unit time ($cm \cdot h^{-1}$); i_1 is the infiltration rate for the first unit time; p is the empirical index which ranges from 0.3 to 0.8 and is based on the soil properties and moisture, and p is initially determined as 0.5 in this study.

Unsaturated hydraulic conductivity (K, $mm \cdot d^{-1}$) is calculated by van Genuchten [38] and van Genuchten and Nielsen [39] (Equations (5) and (6)).

$$K = K_s \left(\frac{\theta - \theta_r}{\theta_s - \theta_r} \right)^{0.5} \left\{ 1 - \left[1 - \left(\frac{\theta - \theta_r}{\theta_s - \theta_r} \right)^{\frac{1}{m}} \right]^m \right\}^2 \quad (5)$$

$$m = 1 - \frac{1}{n} \quad (6)$$

where K_s is the saturated hydraulic conductivity ($mm \cdot d^{-1}$); θ is the soil moisture ($cm^3 \cdot cm^{-3}$); θ_r and θ_s are the residual and saturated soil moistures ($cm^3 \cdot cm^{-3}$) respectively; and m, n are dimensionless empirical parameters. Parameters for Equation (5) were predicted using the Rosetta module [40] based on soil particle size and bulk density (Table 2).

Table 2. Parameters of Equations (5) and (6) for the model. θ_r: residual soil moisture; θ_s: saturated soil moisture.

Depth	θ_r $cm^3 \cdot cm^{-3}$	θ_s $cm^3 \cdot cm^{-3}$	α 1/cm	n -	K_s mm/d
0–10 cm	0.0883	0.4691	0.0082	1.5057	121.9
10–20 cm	0.0919	0.4774	0.0093	1.4737	125.4
20–30 cm	0.0921	0.4776	0.0094	1.4702	125.9
30–40 cm	0.0901	0.4733	0.0087	1.4893	123.5
40–60 cm	0.0763	0.4540	0.0058	1.6156	131.2
60–80 cm	0.0687	0.4477	0.0051	1.6582	176.0
80–100 cm	0.0616	0.4431	0.0046	1.6903	235.6

Notes: θ_r and θ_s are the residual and saturated soil moistures ($cm^3 \cdot cm^{-3}$) respectively; K_s is the saturated hydraulic conductivity ($mm \cdot d^{-1}$); α and n are dimensionless empirical parameters.

If soil moisture in the upper layer (θ) is larger than θs, I (Figure 2, Equations (1)–(3)) from the upper layer to the lower layer is equal to θ − θs; if θ ranges from θr to θs, I is equal to K; otherwise, I = 0.

2.2.3. Groundwater Recharge

Groundwater table (GWT) depths were obtained according to the local water resources bulletin and Liang et al. [41]. More exactly, the GWT depths of study area ranged from 1.14 m (November) to 2.59 m (March) and averaged at 1.82 m in 2012. In 2013 the lowest, deepest and average GWTs were 1.45 m (November), 2.33 m (March) and 1.91 m, respectively.

Groundwater recharge (RW) was calculated based on empirical formula proposed by Li [42] and Du et al. [25].

$$\frac{W_g}{W_c} = -0.54742H + 1.66494 \tag{7}$$

where W_g is available groundwater (mm); W_c is the crop water requirement (mm); and H is the GWT (m).

Distribution of RW in the soil profile was calculated based on Feng and Liu [43] and Chen et al. [44], which was also to be used in the CERES-Wheat model (Equation (8)).

$$w_{i+1}^t = W_g \frac{(\theta_{i+1}^t - \theta_{w\,i+1})h_{i+1} - (\theta_i^t - \theta_{w\,i})h_i}{0.5(h_i + h_{i+1})} \tag{8}$$

where w_{i+1}^t is water flux moving upward from layer i + 1 to layer i by capillarity at time t (mm); θ_{i+1}^t, θ_i^t, θ_{wi+1}, and θ_{wi} are soil moisture and wilting point of layer i + 1 and layer i at time t ($cm^3 \cdot cm^{-3}$); h_i and h_{i+1} are the thicknesses of layer i + 1 and layer i (cm).

2.2.4. Root Distribution

Root distribution was determined according to the researches of Gale and Grigal [45] and Jackson et al. [46] (Equation (9)).

$$Y(z) = 1 - \beta^z \tag{9}$$

where Y(z) is the accumulated root percentage with soil depth (%) and z is the soil depth (100 cm) calculated from surface and the positive direction is downward (cm). β is an empirical parameter affected by plant types, soil and climate conditions. Jackson et al. [46] indicated that β ranges from 0.913 to 0.978; in our study, β was defined as 0.95.

2.2.5. Root Water Uptake

The Feddes et al. [47] model was used to determine root water uptake (RWU) (Equation (10)).

$$RWU = \frac{\alpha(h)}{\int_0^L \alpha(h)dz} T_p \tag{10}$$

where RWU is the root water uptake rate ($mm \cdot d^{-1}$); L is the root depth (100 cm); T_p is the potential transpiration rate ($mm \cdot d^{-1}$); z is the coordinate axis and positive downward (cm); and α(h) is the function about the soil water potential (SWP) (Equation (11)).

$$\alpha(h) = \begin{Bmatrix} \frac{h_1}{h} & , & h \geq h_1 \\ 1 & , & h_2 \leq h < h_1 \\ \frac{h-h_3}{h_2-h_3} & , & h_3 \leq h < h_2 \\ 0 & , & h < h_3 \end{Bmatrix} \tag{11}$$

In Equation (11), h is the soil water potential (cm). h_1, h_2, and h_3 are three threshold values of soil water potential. To be specific, if soil is very wet and has poor ventilation when SWP is higher than h_1,

then RWU decreases with SWP. h_2 is the SWP when plant suffers from water stress and h_3 is the SWP at the wilting point.

Due to the SWP measurements being costly and time consuming, Feddes et al. [48] also proposed that SWP could be replaced by soil moisture (Equation (12)).

$$f(\theta) = \begin{cases} 0 & , \quad \theta \leq \theta_{wilt} \\ \frac{\theta - \theta_{wilt}}{\theta_{stress} - \theta_{wilt}} & , \quad \theta_{wilt} < \theta < \theta_{stress} \\ 1 & , \quad \theta > \theta_{stress} \end{cases} \tag{12}$$

In Equation (12), θ is soil moisture ($cm^3 \cdot cm^{-3}$); θ_{wilt} is the wilting point expressed by moisture ($cm^3 \cdot cm^{-3}$); θ_{stress} is the soil moisture when plant is under water stress ($cm^3 \cdot cm^{-3}$). The details about parameters in Equation (12) are shown in Table 3. More exactly, the ranges of parameters in Equations (10)–(12) were determined according to previous studies [32,49] and the exact parameters value were calibrated based on the soil moisture observations in non-saline treatments using a trial-and-error method, which is a fundamental method of problem solving, characterized by repeated, varied attempts until acceptance of results [50].

Table 3. List of Feddes model parameters.

Parameter	Units	Range	Value	Description	Reference
θ_{wilt}	$cm^3 \cdot cm^{-3}$	0.06–0.10	0.10	Wilting point	[49]
θ_{fc}	$cm^3 \cdot cm^{-3}$	0.32–0.42	0.39	Field capacity	[49]
θ_{stress}	$cm^3 \cdot cm^{-3}$	(0.45–0.9)·θ_{fc}	0.6·θ_{fc}	Stress point	[32]

By considering the root distribution (Section 2.2.4) together, the rate of RWU can be expressed as Equation (13).

$$RWU = T_p \cdot f(\theta) \cdot Y(z) \tag{13}$$

2.2.6. Evapotranspiration and Crop Coefficients (K_c)

Reference evapotranspiration (ET_0) was calculated based on Penman–Monteith equations [16] (Equation (14)).

$$ET_0 = \frac{0.408\Delta(R_n - G) + \gamma \frac{900}{T+273} u_2 (e_s - e_a)}{\Delta + \gamma(1 + 0.34u_2)} \tag{14}$$

where ET_0 is the reference evapotranspiration ($mm \cdot d^{-1}$); R_n is net radiation at the crop surface ($MJ \cdot m^{-2} \cdot d^{-1}$); G is soil heat flux density ($MJ \cdot m^{-2} \cdot d^{-1}$); T is mean daily air temperature at 2-m height (°C); u_2 is wind speed at 2 m height ($m \cdot s^{-1}$); e_s is saturation vapor pressure (kPa); e_a is actual vapor pressure (kPa); $e_s - e_a$ is saturation vapor pressure deficit (kPa); Δ is slope vapor pressure curve ($kPa \cdot °C^{-1}$); and γ is psychrometric constant ($kPa \cdot °C^{-1}$).

Since sunflowers were sown below plastic films (reducing surface evaporation), the single crop coefficient (K_c) method was used to calculated the crop water requirement (ET_c) (Equation (15)).

$$ET_c = K_c \cdot ET_0 = E_p + T_p \tag{15}$$

In Equation (15), E_p and T_p are potential soil evaporation and potential transpiration, respectively ($mm \cdot d^{-1}$). Considering the plastic films that could reduce evaporation and regarding its coefficient as an adjustable parameter (values ranging from 0 to 0.5) [51], and through calibration we chose 0.1 for an appropriate value; thus E_p was determined as in Equation (16).

$$E_p = 0.1 \cdot ET_c \tag{16}$$

Then,

$$T_p = K_c \cdot ET_0 - E_p \tag{17}$$

Sunflower growth periods were divided into four stages (noted as day after sowing (DAS)), initial stage (DAS: 1–36), rapid growth stage (DAS: 37–57), middle stage (DAS: 58–90), and mature stage (DAS: 90–109) according to the study of Du et al. [25] and Allen et al. [16]. Initial K_c values for each stage were 0.3, 0.75, 1.2, and 0.35, respectively [16].

2.2.7. Modeling Process

Soil water flow and water uptake by sunflowers were computed for a soil profile with 100-cm depth. The simulation period extended from the early June to late September, and corresponded to the growth period of sunflowers. First, soil moisture observations in 2012 were used to calibrate the K_c for each stage of sunflowers. In this step, only K_c values were modified and other parameters (e.g., Tables 2 and 3) were not changed because we assumed that the effects of salinity on sunflower growth could be reflected by K_c. Then the local-based K_c values for sunflower growing in the saline soils involving a relationship between K_c of initial stage and soil salinity were proposed. After that, soil moisture observations in 2013 were used to evaluate the proposed local-based K_c values and the contrastive analysis between our K_c values against previously reported research results.

2.3. Statistical Analysis

The determination coefficient (R^2, Equation (18)) and the root-mean-square error (RMSE, Equation (19)) were used to evaluate the model performance.

$$R^2 = \left[\frac{\sum_{i=1}^{n} \left(Y_i^{obs} - \overline{Y}_i^{obs} \right) \left(Y_i^{sim} - \overline{Y}_i^{sim} \right)}{\sqrt{\sum_{i=1}^{n} \left(Y_i^{obs} - \overline{Y}_i^{obs} \right)^2} \sqrt{\sum_{i=1}^{n} \left(Y_i^{sim} - \overline{Y}_i^{sim} \right)^2}} \right]^2 \quad (18)$$

$$RMSE = \sqrt{\frac{\sum_{i=1}^{n} \left(Y_i^{obs} - Y_i^{sim} \right)^2}{n}} \quad (19)$$

where Y_i^{obs} is the ith observed value, Y_i^{sim} is the ith simulated value, and $\overline{Y_i^{obs}}$ and $\overline{Y_i^{sim}}$ are the means of the observed and simulated values, respectively.

3. Results

3.1. Meteorological Conditions

The daily precipitation measured by the field meteorological station of the experiment station from April to October in 2012 and 2013 varied from 0–67.2 mm·d^{-1} to 0–20.8 mm·d^{-1}, respectively, with an accumulated precipitation of 254 mm for 2012 and 64.8 mm for 2013 (Figure 3), which indicated that the year 2012 was much wetter than 2013. Furthermore, the local water resources bulletin also confirmed that the 2012 was a wet year while 2013 was a drier one. Specifically, the total precipitation of 2012 in our experiment station is 400.6 mm (from April to October), which was about 127.6% higher than the historical mean precipitation (176 mm). Meanwhile, the total precipitation of 2013 was only about half of the historical mean precipitation. Inversely, calculated ET_0 values in 2012 were relative smaller than those in 2013 according to the accumulated ET_0 during the sunflower growth stages (Figure 3). The different weather conditions of 2012 and 2013 increased the challenge for model calibration and evaluation but could also prove an indication of the stability of the model, if it could perform accurately in both years.

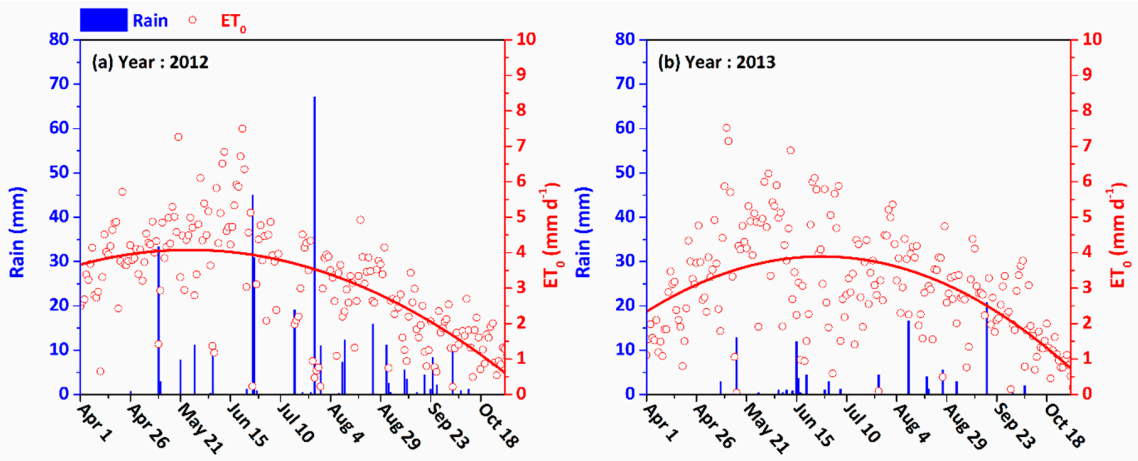

Figure 3. Precipitation and potential evapotranspiration (ET_0) of sunflower growing seasons in 2012 (**a**) and 2013 (**b**). Red curves are the parabolic fitting of the ET_0.

3.2. Calibration of the WFSP Model

Soil water flow and water uptake by sunflower were computed for a soil profile with 100-cm depth. The simulation period was from early June to late September, and conceded with the growth period of sunflowers. Model setup required specific daily precipitation and reference evapotranspiration as input data. The parameter calibration analysis was carried out using the main factors affecting the water regime (i.e., soil moisture, the cumulative values of actual transpiration and evaporation, capillary rise and other additional parameters) as the objective variables. After that, the above-mentioned sensitive parameters and some parameters introduced in Section 2.2 were calibrated using a trial-and-error method. An iterative calibration approach was adopted to account for the interactions between the measured soil moisture and simulated soil moisture. After proper calibration, the model was considered to be adequate for the evaluation of water movement in the soil-plant-atmosphere continuum (SPAC) system. The observed soil water contents in different soil layers relative to 2012 and 2013 were used to calibrate and validate the model, respectively. To assess the performance of the model, several goodness-of-fit indicators proposed in Section 2.3 were used as in the paper (e.g., R^2 and RMSE). Based on the parameter sensitivity analysis, many parameters were only slightly adjusted depending on the goodness-of-fit indicators. The root water uptake parameters, including Feddes' parameters and the basic soil parameters for sunflowers were calibrated and were shown in the former section. Some calibrated K_c values for sunflowers were slightly lower than those recommended in literature. This may due to the fact that the crop varieties planted in Hetao Irrigation District were more salt-tolerant than in the non-salinized area.

Soil moisture observed at different sunflower growth stages were well captured by the WFSP model except for the surface soil (0–5 cm) in the model calibration process (Figure 4, Year 2012). More exactly, R^2 in initial, rapid growth, middle, and mature stages for 5–100 cm depth were 0.60, 0.61, 0.66, and 0.72 respectively while RMSE were only 0.07, 0.04, 0.07 and 0.09 $cm^3 \cdot cm^{-3}$ respectively.

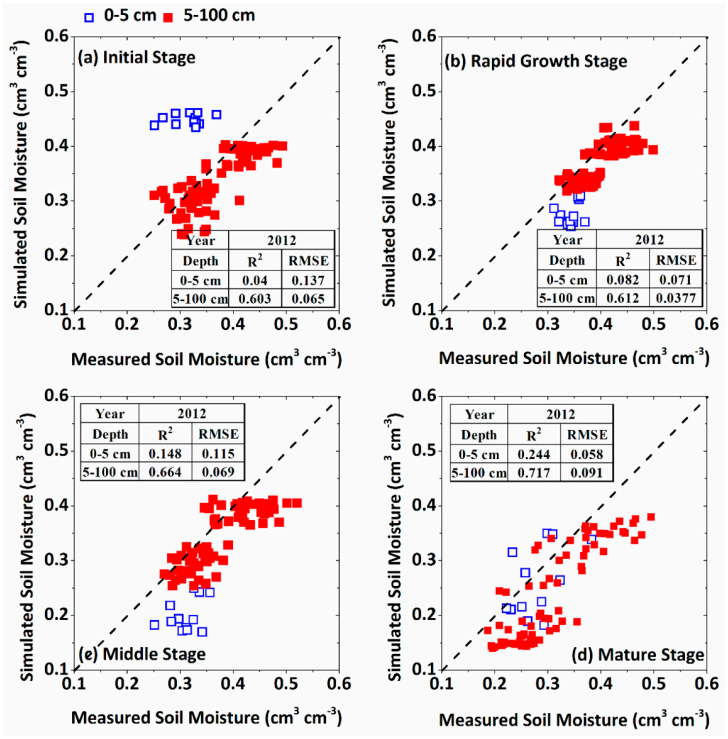

Figure 4. Soil moisture simulation of sunflowers at four different growth stages of model calibration using the observations in 2012 ((**a**): initial stage; (**b**): rapid growth stage; (**c**): middle stage; (**d**): mature stage; blue points indicate observations in 0–5 cm and red points indicate observations in 5–100 cm). RMSE: root-mean-square error.

Accumulative evapotranspiration (AETc) was also calculated, and the average AETc of the four growth stages were 77.1, 66.5, 156.2, and 44.3 mm respectively in 2012 (Figure 5a); and 60.0, 74.2, 123.6, and 19.7 mm respectively in 2013 (Figure 5b), indicating that the AETc of sunflowers was comparable in first two growth stages and achieved highest and lowest values in the middle and mature stages respectively.

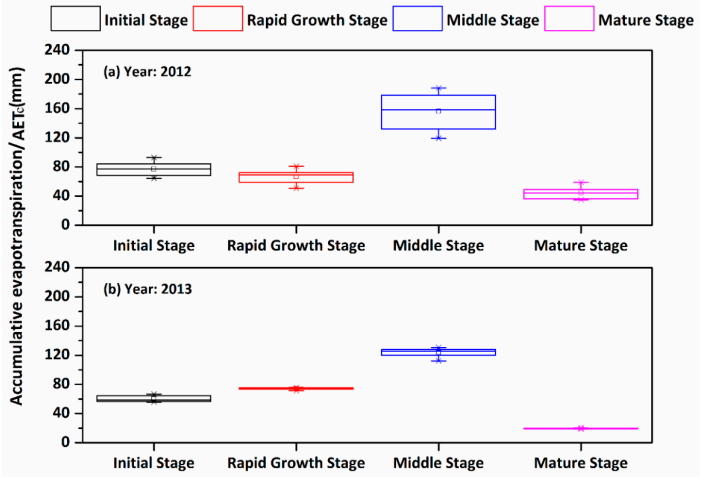

Figure 5. Box plot of accumulative evapotranspiration (AETc) of the four growth stages of sunflowers in 2012 (**a**) and 2013 (**b**) respectively. The line in the box is the median, the edges of the box are the lower hinge (25%, Q1) and the upper hinge (75%, Q3), the up and low boundary lines out of the box indicate the maximum and minimum values and the cross symbols near the up and low boundaries are the 99% and 1% hinges respectively.

3.3. Establishment and Evaluation of the Locally-Based Sunflower K_c Values

Calibration of the WFSP model also indicates that K_c values for sunflowers in saline soils (EC_e = 3.3–18.5 dS·m^{-1}) ranged from 0.25–0.37, 0.51–0.86, 0.80–1.49, and 0.11–0.73 of initial (K_{c1}), rapid growth (K_{c2}), middle (K_{c3}), and mature stages (K_{c4}) respectively. Meanwhile, linear regression analysis indicated that all K_c values except K_{c1} decreased with soil salinity levels (Figure 6). Furthermore, K_{c1} had a very good linear correlation with the initial salinity level of 0–20 cm depth (Equation (20)).

$$K_{c1} = 0.0059EC_e + 0.2401 \quad (20)$$

Therefore, we assume that sunflower's K_{c1} value in saline soils could be easily obtained through Equation (20) while the locally-based K_c values for another three stages could be 0.51–0.86, 0.80–1.49, and 0.11–0.73 for use as reference values. To further simplify, we averaged the K_{c2}, K_{c3}, and K_{c4} values obtained in our model (0.659, 1.156, and 0.324, respectively) and applied the WFSP model to evaluate their accuracy with the calculated K_{c1} value (Equation (20)) using soil and weather conditions in 2013 (Figure 7). Similar to the model calibration process, higher accuracies for soil moisture simulations were also obtained for all four growth stages when the surface soils were ignored (0–10 cm in 2013). More exactly, R^2 in the initial, rapid growth, middle, and mature stages for 10–100-cm depth were 0.66, 0.68, 0.56, and 0.58, respectively, while RMSEs were only 0.04, 0.04, 0.08 and 0.11 cm^3·cm^{-3}, respectively.

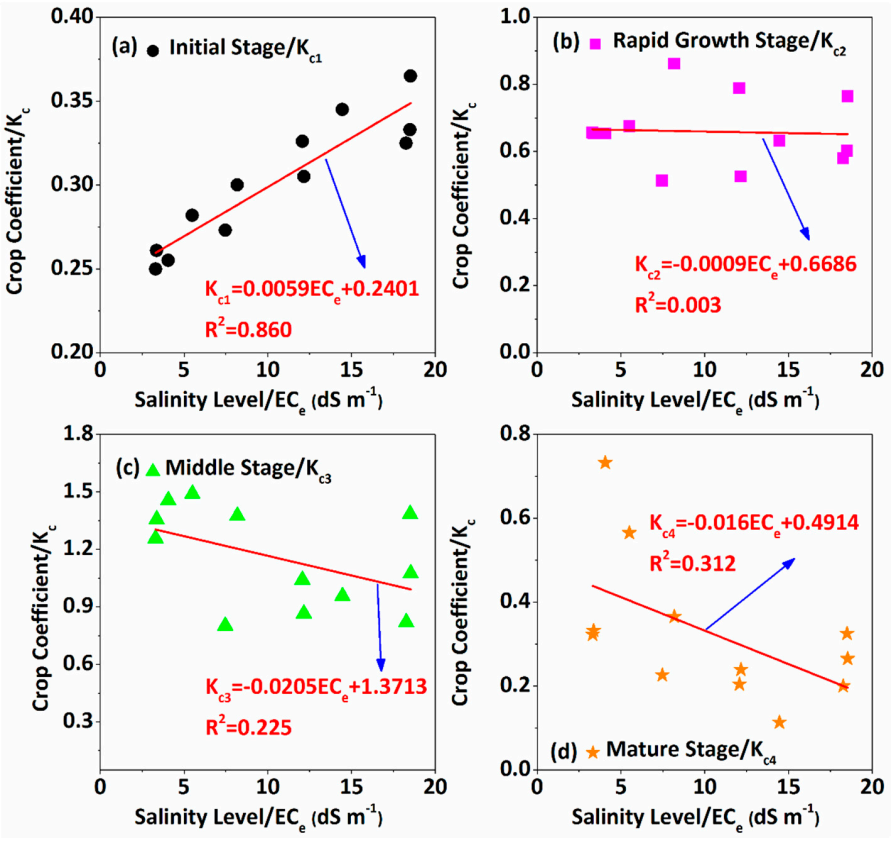

Figure 6. The relationship between the crop coefficient/K_c of sunflowers simulated by WFSP model and initial salinity level/EC_e (dS·m^{-1}) of 0–20 cm depth.

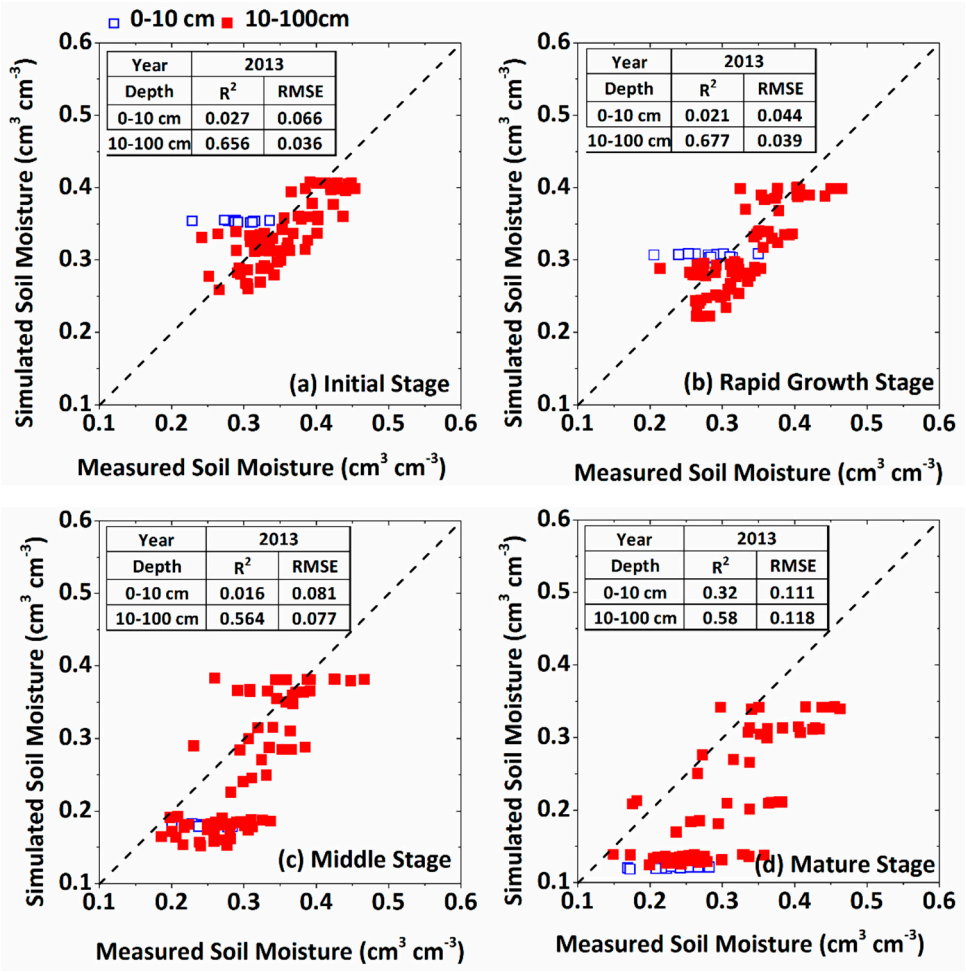

Figure 7. Soil moisture simulation of sunflowers in four different growth stages for model evaluation using the observations in 2013 ((**a**): initial stage; (**b**): rapid growth stage; (**c**): middle stage; (**d**): mature stage; blue points indicate observations in 0–10 cm and red points indicate observations in 10–100 cm).

4. Discussion

4.1. Performance of the WFSP Model

Different from other models (e.g., HYDRUS) which use Richards equation to describe soil water flow [52,53], the WFSP model calculated water movement in the soil-plant system based on the water balance principle. The method is simpler than others and can overcome the iterative convergence issue when solving the Richards equation [54,55]. In our study, the WFSP model could simulate soil water dynamics accurately in both 2012 and 2013 except for the surface soils (Figures 4 and 7, $R^2 > 0.56$, RMSE < 0.1 $cm^3 \cdot cm^{-3}$). Meanwhile, the AETc values for the different growth stages of the sunflower calculated by the WFSP model were also similar to those in research by Ren et al. [56], Du et al. [25], and Xin et al. [57]. Therefore, the WFSP model could obtain reasonable simulations of soil water flow in the soil–plant system and could be used as a tool for analyzing the agro-hydrological processes and inverting the sunflower crop coefficient under salt stress. However, the poor accuracy for surface soil moisture simulation may be caused by the unusual weather conditions in 2012. In addition, the uncertainties of input data and field measurements such as groundwater table [58], the possible preferential flow [59] and even the observation errors might also bring adverse influences on the accuracy of the simulations for all four stages.

4.2. Sunflower's K_c Values in Saline Soils

Crop coefficient (K_c) is a key parameter for estimating crop water use and to schedule irrigations [12]. In our study, K_c in the initial stage (K_{c1}) was determined by initial soil salinity of 0–20 cm depth due to a very high correlation (R^2 = 0.86, Figure 6a). For the rapid growth, middle and mature stages, sunflower's K_c were 0.659, 1.156, and 0.324, respectively. However, locally-based K_c values for sunflowers in saline soils proposed in our study (LK_c) were different to previous research (Table 4). FAO-56 reported K_c values were 0.35, 1.0–1.15, and 0.35 for initial, middle and mature stages of sunflowers respectively [16]. LK_c used four growth stages and were adjusted a little (<8%) in middle and mature stages, which increased R^2 of soil moisture simulation (10–100 cm) for about 10% (Table 4) in moderately salinized soil (EC_e = 9.44 dS·m^{-1}). In India, Tyagi et al. [20] reported K_c values for sunflowers as 0.52, 1.1, 0.32 and 0.41, estimating K_c values 11.6%–74.2% higher than the values suggested by FAO-56, also different to our LK_c values. Even for the same plants in close areas, K_c values may also be extremely different. In Hetao Irrigation District, Dai et al. [60] reported K_c values of 0.697, 0.751, 0.804, and 0.35, respectively for the four growth stages, with K_c values over 100% higher than ours in the initial stage, and about 30% lower in the middle stage. Du et al. [25] also obtained different K_c values for sunflowers compared to both Dai et al. [60] and our results (Table 4). The differences among K_c values might be caused from both soil and climate conditions and one of the most important factors was soil salinity [61,62]. Taking FAO-56 as an example, it deals with the calculation of crop evapotranspiration (ET_c) under standard conditions. The values for K_c in FAO-56 are values for non-stressed crops cultivated under excellent agronomic and water management conditions and achieving maximum crop yield (standard conditions). Meanwhile, FAO-56 also ignores the difference among varieties. In addition, some specific agricultural practices such as plastic film covering the soil surface might also impact Kc determination. Therefore, FAO-56 strongly encouraged users to obtain appropriate local K_c values for a specific crop variety based on local soil and weather conditions. By considering salinity effects, LK_c values obtained the highest accuracy for soil moisture simulation (R^2 = 0.7) in moderately salinized soils when compared to previous research (Table 4).

Table 4. Comparison of crop coefficients/K_c between different researchers and our model in moderately salinized soil (EC_e = 9.44 dS·m^{-1}).

Item	Initial Stage	Rapid Growth Stage	Middle Stage	Mature Stage	R^2	Location	Reference
1	0.52	1.1	1.32	0.41	0.55	Karnal, India (29°43′ N, 76°58′ E)	[20]
2	0.697	0.751	0.804	0.35	0.55	Dengkou County, Hetao (40°24′ N, 107°02′ E)	[60]
3	0.194	0.779	1.26	0.315	0.67	Linhe County, Hetao (40°43′ N, 76°58′ E)	[25]
4	0.14	—	1.08	0.24	0.66	Yangchang, Hetao (40°48′ N, 107°05′ E)	[56]
5	0.35	—	1–1.15	0.35	0.64	California, US	[16]
6	Equation (20)	0.659	1.156	0.324	0.7	Wuyuan County, Hetao (41°04′ N, 108°00′ E)	WFSP model

In general, higher soil salinity results in lower K_c, which is also in accordance with our K_{c2}, K_{c3}, and K_{c4} (Figure 6b–d). However, a very high positive correlation was found between K_{c1} and salinity level (Figure 6a), which was unusual but also demonstrated that effects of salinity on K_{c1} were more pronounced than in other stages. Similar results also obtained by Grattan and Grieve [63], who indicated that the initial stage of the crop was generally more salt sensitive than later growth stages and that crop failures during initial stages are common on saline lands. However, Bernstein and Hayward [64] reported that salt accumulations at seed depths are often much greater than at lower levels in the soil profile and when response to actual ambient salinity is considered, the initial stage is generally no more salt sensitive than later stages. Meanwhile, sunflowers were classified as moderately salt-tolerant plants by Katerji et al. [65] and previous studies also proved that a certain

extent of salinity level might enhance sunflower growth [66]. Therefore, it is reasonable to believe that two or more of these processes with respect to the positive or negative effects of salinity on sunflowers may occur at the initial stage, but whether they ultimately affect K_c value or crop yield depends upon the salinity level, composition of salts, the crop species, and some other environmental factors which need further research.

5. Conclusions

Crop evapotranspiration calculation (ET_c) plays a pivotal role in evaluating irrigation management strategies for improving agricultural water use, especially in saline regions. Appropriate irrigation schedules are of vital importance to adequately manage it. To determine ETc and make appropriate irrigation schedules, crop coefficients (K_c) have to be representatively determined. Based on soil moisture observations, a strong dynamics analysis tool (Vensim software) was used to establish and develop a physically-based model (WFSP model) for estimating the crop coefficients (K_c) of sunflowers in the Hetao Irrigation District. The two main findings were that firstly, only soil moisture data is needed for WFSP model, which makes this method more practical for developing an irrigation schedule. Meanwhile, the WFSP model could estimate reasonable simulations on the soil water flow in the soil–plant system and thus could be used as a tool for analyzing the agro-hydrological processes and deducing the sunflower crop coefficient under salt stress conditions. Secondly, our study indicates that the effects of salt stress on plant could be considered with K_c determination. K_{c1} had a very good linear correlation with the initial salinity level of 0–20 cm depth (Equation (20)), and local-based K_c values for rapid growth, middle, and mature stages are recommended as 0.659, 1.156, and 0.324, respectively. These local crop coefficients could be very useful in irrigation schedules for local agricultural water managers.

However, there are still several shortcomings of our study. Firstly, soil salt dynamics were not considered in the study and further work should focus on the effects of salt dynamics with respect to K_c at the different crop stages. In addition, EC_e was used to reflect the total salt content and the effects of salt composition on K_c and would need further study. Meanwhile, the LK_c values for sunflowers, especially Equation (20) also need to be evaluated in other saline soils to test their stability and applicability.

Acknowledgments: This work was made possible by support from the State Natural Science Fund of China (Grant Nos. 51609175 and 51379151), Open Foundation of State Key Laboratory of Hydrology-Water Resources and Hydraulic Engineering (Grant No. 2015490211), the Fundamental Research Funds for the Central Universities (Grant Nos. 2042016kf0043 and 2042016kf1034), and the China Postdoctoral Science Foundation (Grant No. 2015M582274). Authors appreciate Yonggen Zhang's help for proofreading the manuscript.

Author Contributions: The research present here was carried out in collaboration between all authors. Wenzhi Zeng, Minghai Hong and Jiesheng Huang conceived the idea and designed the study; Minghai Hong carried out the data analysis, set up the model, and prepared the first draft of the manuscript; Wenzhi Zeng and Yuanhao Fang were also of vital importance in revising the manuscript; and Tao Ma, Guoqing Lei, Yuanyuan Zha, Jingwei Wu and Jiesheng Huang provided important advice on the concept writing of the manuscript and English grammar.

Conflicts of Interest: The authors declare no conflict of interest.

References

1. Demir, A.O.; Goksoy, A.T.; Buyukcangaz, H.; Turan, Z.M.; Koksal, E.S. Deficit irrigation of sunflower (*Helianthus annuus* L.) in a sub-humid climate. *Irrig. Sci.* **2006**, *24*, 279–289. [CrossRef]
2. Shi, H.; Akae, A.; Kong, D.; Zhang, L.; Chen, Y.; Wei, Z.; Li, Y.; Zhang, Y. In study on sunflower response to soil water and salt stress in the Hetao area, China. In *Water-Saving Agriculture and Sustainable use of Water and Land Resources*; Shaanxi Science and Technology Press: Xi'an, China, 2003; pp. 111–116.
3. Feng, Z.Z.; Wang, X.K.; Feng, Z.W. Soil n and salinity leaching after the autumn irrigation and its impact on groundwater in Hetao irrigation district, China. *Agric. Water Manag.* **2005**, *71*, 131–143. [CrossRef]
4. Li, L.; Shi, H.; Wang, C.; Liu, H. Simulation of water and salt transport of uncultivated land in Hetao irrigation district in Inner Mongolia. *Trans. Chin. Soc. Agric. Eng.* **2010**, *26*, 31–35.

5. Ertek, A.; Kara, B. Yield and quality of sweet corn under deficit irrigation. *Agric. Water Manag.* **2013**, *129*, 138–144. [CrossRef]
6. Cakir, R. Effect of water stress at different development stages on vegetative and reproductive growth of corn. *Field Crop Res.* **2004**, *89*, 1–16. [CrossRef]
7. Dagdelen, N.; Yilmaz, E.; Sezgin, F.; Gurbuz, T. Water-yield relation and water use efficiency of cotton (*Gossypium hirsutum* L.) and second crop corn (*Zea mays* L.) in western Turkey. *Agric. Water Manag.* **2006**, *82*, 63–85. [CrossRef]
8. Irmak, S.; Djaman, K.; Rudnick, D.R. Effect of full and limited irrigation amount and frequency on subsurface drip-irrigated maize evapotranspiration, yield, water use efficiency and yield response factors. *Irrig. Sci.* **2016**, *34*, 271–286. [CrossRef]
9. Kiziloglu, F.M.; Sahin, U.; Kuslu, Y.; Tunc, T. Determining water-yield relationship, water use efficiency, crop and pan coefficients for silage maize in a semiarid region. *Irrig. Sci.* **2009**, *27*, 129–137. [CrossRef]
10. Payero, J.O.; Melvin, S.R.; Irmak, S.; Tarkalson, D. Yield response of corn to deficit irrigation in a semiarid climate. *Agric. Water Manag.* **2006**, *84*, 101–112. [CrossRef]
11. Zeng, W.Z.; Xu, C.; Wu, J.W.; Huang, J.S. Soil salt leaching under different irrigation regimes: HYDRUS-1D modelling and analysis. *J. Arid Land* **2014**, *6*, 44–58. [CrossRef]
12. Alcaras, L.M.A.; Rousseaux, M.C.; Searles, P.S. Responses of several soil and plant indicators to post-harvest regulated deficit irrigation in olive trees and their potential for irrigation scheduling. *Agric. Water Manag.* **2016**, *171*, 10–20. [CrossRef]
13. Pereira, L.S.; Allen, R.G.; Smith, M.; Raes, D. Crop evapotranspiration estimation with FAO56: Past and future. *Agric. Water Manag.* **2015**, *147*, 4–20. [CrossRef]
14. Vellidis, G.; Tucker, M.; Perry, C.; Wen, C.; Bednarz, C. A real-time wireless smart sensor array for scheduling irrigation. *Comput. Electron. Agric.* **2008**, *61*, 44–50. [CrossRef]
15. Jones, H.G. Irrigation scheduling: Advantages and pitfalls of plant-based methods. *J. Exp. Bot.* **2004**, *55*, 2427–2436. [CrossRef] [PubMed]
16. Allen, R.G.; Pereira, L.S.; Raes, D.; Smith, M. *Crop Evapotranspiration-guidelines for Computing Crop Water Requirements-FAO Irrigation and Drainage Paper 56*; FAO: Rome, Italy, 1998; p. D05109.
17. Jensen, M.E. Water consumption by agricultural plants (Chapter 1). In *Plant Water Consumption and Response. Water Deficits and Plant Growth*; Academic Press: New York, NY, USA, 1968; Volume II, pp. 1–22.
18. Howell, T.A.; Evett, S.R.; Tolk, J.A.; Copeland, K.S.; Marek, T.H. Evapotranspiration, water productivity and crop coefficients for irrigated sunflower in the US southern high plains. *Agric. Water Manag.* **2015**, *162*, 33–46. [CrossRef]
19. Reddy, K.C.; Arunajyothy, S.; Mallikarjuna, P. Crop coefficients of some selected crops of Andhra Pradesh. *J. Inst. Eng. (India): Ser. A* **2015**, *96*, 123–130. [CrossRef]
20. Tyagi, N.K.; Sharma, D.K.; Luthra, S.K. Determination of evapotranspiration and crop coefficients of rice and sunflower with lysimeter. *Agric. Water Manag.* **2000**, *45*, 41–54. [CrossRef]
21. Zeng, W.Z.; Xu, C.; Huang, J.S.; Wu, J.W.; Ma, T. Emergence rate, yield, and nitrogen-use efficiency of sunflowers (*Helianthus annuus*) vary with soil salinity and amount of nitrogen applied. *Commun. Soil Sci. Plant Anal.* **2015**, *46*, 1006–1023. [CrossRef]
22. Zeng, W.Z.; Xu, C.; Wu, J.W.; Huang, J.S.; Zhao, Q.; Wu, M.S. Impacts of salinity and nitrogen on the photosynthetic rate and growth of sunflowers (*Helianthus annuus* L.). *Pedosphere* **2014**, *24*, 635–644. [CrossRef]
23. Zeng, W.Z.; Wu, J.W.; Hoffmann, M.P.; Xu, C.; Ma, T.; Huang, J.S. Testing the apsim sunflower model on saline soils of Inner Mongolia, China. *Field Crop Res.* **2016**, *192*, 42–54. [CrossRef]
24. Bhantana, P.; Lazarovitch, N. Evapotranspiration, crop coefficient and growth of two young pomegranate (*Punica granatum* L.) varieties under salt stress. *Agric. Water Manag.* **2010**, *97*, 715–722. [CrossRef]
25. Du, B.; Qu, Z.; Yu, J.; Sun, G.; Shi, J. Experimental study on crop coefficient under mulched drip irrigation in Hetao irrigation district of Inner Mongolia. *J. Irrig. Drain.* **2014**, *33*, 16–20.
26. Miller, W.P.; Miller, D.M. A micro-pipette method for soil mechanical analysis. *Commun. Soil Sci. Plant Anal.* **1987**, *18*, 1–15. [CrossRef]
27. Bao, S.D. *Soil Agro-Chemistrical Analysis*, 3rd ed.; China Agriculture Press: Beijing, China, 2011; p. 496.
28. Institute of Soil Science. *Analysis of Soil Physico-Chemical Properties*; Shanghai Scientific & Technical Publishers: Shanghai, China, 1978.
29. Forrester, J.W. Industrial dynamics: A major breakthrough for decision makers. *Harv. Bus. Rev.* **1958**, 37–66.

30. Forrester, J.W. *Industrial Dynamics*; MIT Press: Cambridge, UK, 1961.
31. Khan, S.; Luo, Y.F.; Ahmad, A. Analysing complex behaviour of hydrological systems through a system dynamics approach. *Environ. Modell. Softw.* **2009**, *24*, 1363–1372. [CrossRef]
32. Miller, G.R.; Cable, J.M.; McDonald, A.K.; Bond, B.; Franz, T.E.; Wang, L.X.; Gou, S.; Tyler, A.P.; Zou, C.B.; Scott, R.L. Understanding ecohydrological connectivity in savannas: A system dynamics modelling approach. *Ecohydrology* **2012**, *5*, 200–220. [CrossRef]
33. Yang, C.-C.; Chang, L.-C.; Ho, C.-C. Application of system dynamics with impact analysis to solve the problem of water shortages in Taiwan. *Water Resour. Manag.* **2008**, *22*, 1561–1577. [CrossRef]
34. Eberlein, R.L.; Peterson, D.W. Understanding models with Vensim™. *Eur. J. Oper. Res.* **1992**, *59*, 216–219. [CrossRef]
35. Systems, V. *Vensim Reference Mannual*; Ventana Systems: Harvard, MA, USA, 2007.
36. Systems, V. *Vensim Version 5 User's Guide*; Ventana Systems: Harvard, MA, USA, 2007.
37. Igboekwe, M.U.; Adindu, R.U. Use of Kostiakov's Infiltration Model on Michael Okpara University of Agriculture, Umudike Soils, Southeastern, Nigeria. *J. Water Resour. Prot.* **2014**, *6*, 888–894. [CrossRef]
38. Vangenuchten, M.T. A closed-form equation for predicting the hydraulic conductivity of unsaturated soils. *Soil Sci. Soc. Am. J.* **1980**, *44*, 892–898. [CrossRef]
39. Vangenuchten, M.T.; Nielsen, D.R. On describing and predicting the hydraulic-properties of unsaturated soils. *Ann. Geophys.* **1985**, *3*, 615–627.
40. Schaap, M.G.; Leij, F.J.; van Genuchten, M.T. ROSETTA: A computer program for estimating soil hydraulic parameters with hierarchical pedotransfer functions. *J. Hydrol.* **2001**, *251*, 163–176. [CrossRef]
41. Liang, J.; Li, R.; Shi, H.; Li, Z.; Lu, X.; Bu, H. Effect of mulching on transfer and distribution of salinizated soil nutrient in Hetao irrigation district. *Trans. Chin. Soc. Agric. Mach.* **2016**, *2*, 113–121.
42. Li, F. Experimental study of groudwater availability in relation to crops. *Groundwater* **1992**, 197–202.
43. Feng, G.; Liu, C. Analysis of root system growth in relation to soil water extraction pattern by winter wheat under water-limiting conditions. *J. Nat. Resour.* **1998**, *3*, 234–241.
44. Chen, H.; Gao, Z.; Wang, S.; Hu, Y. Modeling on impacts of climate change and human activities variability on the shallow groundwater level using modflow. *J. Hydraul. Eng.* **2012**, *43*, 344–353.
45. Gale, M.R.; Grigal, D.F. Vertical root distributions of northern tree species in relation to successional status. *Can. J. For. Res.* **1987**, *17*, 829–834. [CrossRef]
46. Jackson, R.B.; Canadell, J.; Ehleringer, J.R.; Mooney, H.A.; Sala, O.E.; Schulze, E.D. A global analysis of root distributions for terrestrial biomes. *Oecologia* **1996**, *108*, 389–411. [CrossRef]
47. Feddes, R.A.; Kowalik, P.J.; Zaradny, H. Simulation of field water use and crop yield. *Soil Sci.* **1980**, *129*, 193.
48. Feddes, R.A.; Kowalik, P.; Kolinska-Malinka, K.; Zaradny, H. Simulation of field water uptake by plants using a soil water dependent root extraction function. *J. Hydrol.* **1976**, *31*, 13–26. [CrossRef]
49. Zhang, M.; Shi, X. *Soil and Crop Science*; China Water & Power Press: Beijing, China, 2012.
50. Putnam, H. Trial and error predicates and the solution to a problem of Mostowski. *J. Symb. Logic* **1965**, *30*, 49–57. [CrossRef]
51. Yuting, Y.; Songhao, S. Comparison of dual-source evapotranspiration models in estimating potential evaporation and transpiration. *Trans. Chin. Soc. Agric. Eng.* **2012**, *28*, 85–91.
52. Šimůnek, J.; Van Genuchten, M.T.; Sejna, M. *The Hydrus-1d Software Package for Simulating the Movement of Water, Heat, and Multiple Solutes in Variably Saturated Media, Version 3.0, Hydrus Software Series 1*; Department of Environmental Sciences, University of California Riverside: Riverside, CA, USA, 2005.
53. Zhang, Z.Y.; Wang, W.K.; Yeh, T.C.J.; Chen, L.; Wang, Z.F.; Duan, L.; An, K.D.; Gong, C.C. Finite analytic method based on mixed-form richards' equation for simulating water flow in vadose zone. *J. Hydrol.* **2016**, *537*, 146–156. [CrossRef]
54. Zha, Y.Y.; Shi, L.S.; Ye, M.; Yang, J.Z. A generalized ross method for two- and three-dimensional variably saturated flow. *Adv. Water Resour.* **2013**, *54*, 67–77. [CrossRef]
55. Zha, Y.Y.; Yang, J.Z.; Shi, L.S.; Song, X.H. Simulating one-dimensional unsaturated flow in heterogeneous soils with water content-based richards equation. *Vadose Zone J.* **2013**, *12*, 1–13. [CrossRef]
56. Ren, D.; Xu, X.; Hao, Y.; Huang, G. Modeling and assessing field irrigation water use in a canal system of Hetao, upper Yellow River basin: Application to maize, sunflower and watermelon. *J. Hydrol.* **2016**, *532*, 122–139. [CrossRef]

57. He, X.; Yang, P.L.; Ren, S.M.; Li, Y.K.; Jiang, G.Y.; Li, L.H. Quantitative response of oil sunflower yield to evapotranspiration and soil salinity with saline water irrigation. *Int. J. Agric. Biol. Eng.* **2016**, *9*, 63–73.
58. Sun, M.; Zhang, X.; Huo, Z.; Feng, S.; Huang, G.; Mao, X. Uncertainty and sensitivity assessments of an agricultural–hydrological model (RZWQM2) using the GLUE method. *J. Hydrol.* **2016**, *534*, 19–30. [CrossRef]
59. Wiekenkamp, I.; Huisman, J.A.; Bogena, H.R.; Lin, H.S.; Vereecken, H. Spatial and temporal occurrence of preferential flow in a forested headwater catchment. *J. Hydrol.* **2016**, *534*, 139–149. [CrossRef]
60. Dai, J.; Shi, H.; Tian, D.; Xia, Y.; Li, M. Determined of crop coefficients of main grain and oil crops in Inner Mongolia Hetao irrigated area. *J. Irrig. Drain.* **2011**, 23–27.
61. Homaee, M.; Dirksen, C.; Feddes, R.A. Simulation of root water uptake: I. Non-uniform transient salinity using different macroscopic reduction functions. *Agric. Water Manag.* **2002**, *57*, 89–109. [CrossRef]
62. Skaggs, T.H.; van Genuchten, M.T.; Shouse, P.J.; Poss, J.A. Macroscopic approaches to root water uptake as a function of water and salinity stress. *Agric. Water Manag.* **2006**, *86*, 140–149. [CrossRef]
63. Grattan, S.R.; Grieve, C.M. Salinity mineral nutrient relations in horticultural crops. *Sci. Hortic-Amst.* **1999**, *78*, 127–157. [CrossRef]
64. Bernstein, L.; Hayward, H. Physiology of salt tolerance. *Annu. Rev. Plant Physiol.* **1958**, *9*, 25–46. [CrossRef]
65. Katerji, N.; van Hoorn, J.W.; Hamdy, A.; Mastrorilli, M. Salt tolerance classification of crops according to soil salinity and to water stress day index. *Agric. Water Manag.* **2000**, *43*, 99–109. [CrossRef]
66. Zeng, W.Z. *Research and Simulation for the Coupling Effects of Water, Nitrogen, and Salt on Sunflower*; Wuhan University: Wuhan, China, 2015.